International Journal of Fluid Mechanics & Thermal Sciences
2020; 6(4): 124-131
http://www.sciencepublishinggroup.com/j/ijfmts
doi: 10.11648/j.ijfmts.20200604.13
ISSN: 2469-8105 (Print); ISSN: 2469-8113 (Online)

Review Ariticle

Effect of Anisotropic Permeability on Thermosolutal Convection in a Porous Cavity Saturated by a Non-newtonian Fluid

Yovogan Julien[1, *], Fagbemi Latif[2], Koube Bocco Sèlidji Marius[3], Kouke Dieudonné[2], Degan Gérard[1]

[1]Department of the Energizing Genius and Environment, National University of Sciences, Technologies, Engineering and Mathematics (UNSTIM), Abomey, Republic of Benin

[2]Department of Renewable Energy and Energizing System, University of Abomey Calavi, Abomey Calavi, Republic of Benin

[3]Department of Physics, National University of Sciences, Technologies, Engineering and Mathematics (UNSTIM), Abomey, Republic of Benin

Email address:
julienyovo72@gmail.com (Y. Julien), latiff08@yahoo.fr (F. Latif), koubeco@gmail (K. B. S. Marius), donne.k@aress.solar (K. Dieudonné), ger_degan@yahoofr (D. Gérard)
[*]Corresponding author

To cite this article:
Yovogan Julien, Fagbemi Latif, Koube Bocco Sèlidji Marius, Kouke Dieudonné, Degan Gérard. Effect of Anisotropic Permeability on Thermosolutal Convection in a Porous Cavity Saturated by a Non-newtonian Fluid. *International Journal of Fluid Mechanics & Thermal Sciences*. Vol. 6, No. 4, 2020, pp.124-131. doi: 10.11648/j.ijfmts.20200604.13

Received: November 13, 2020; **Accepted**: November 30, 2020; **Published**: December 16, 2020

Abstract: In this paper, an analytical study is reported on double-diffusive natural convection in a shallow porous cavity saturated with a non-Newtonian fluid by using the Darcy model with the Boussinesq approximations. A Cartesian coordinate system is chosen with the x- and y- axes at the geometrical center of the cavity and the y'-axis vertically upward. The top and bottom horizontal boundaries are subject to constant heat (q) and mass (j) fluxes. The porous medium is anisotropic in permeability whose principal axes are oriented in a direction that is oblique to the gravity vector. The permeabilities along the two principal axes of the porous matrix are denoted by K1 and K2. The anisotropy of the porous layer is characterized by the permeability ratio $K^*=K_1/K_2$ and the orientation angle φ, defined as the angle between the horizontal direction and the principal axis with the permeability K2. The viscous dissipations are negligible. Based on parallel flow approximation theory, the problem is solved analytically, in the limit of a thin layer and documented the effects of the physical parameters describing this investigation. Solutions for the flow fields, Nusselt and Sherwood numbers are obtained explicitly in terms of the governing parameters of the problem.

Keywords: Heat Transfer, Mass Transfer, Isotropy, Anisotropy

1. Introduction

Double-diffusive, or thermosolutal, natural convection is a fluid motion due to simultaneous variations of temperature and concentration in the gravity field. Thermodiffusion in different fluids is a subject of intensive research due to its wide range of applications in many engineering and technological areas, including chemical engineering (deposition of thin films, roll-over in storage tanks containing liquefied natural gas, solution mining of salt caverns for crude oil storage), solid-state physics (solidification of binary alloy and crystal growth), oceanography (melting and cooling near ice surfaces, sea water intrusion into freshwater lakes and the formation of layered or columnar structures during crystallization of igneous intrusions in the Earth's crust), geo-physics (dispersion of dissolvent materials or particulate matter in flows), etc. Non-Newtonian flows are of importance and very present in many industrial processes such as paper making, oil drilling, slurry transporting, food processing, polymer engineering and many others. Some of these processes are discussed by Jaluria [1].

There are very few investigations dealing with double-diffusion convection inside rectangular enclosures confining non-Newtonian fluids. Among them are those performed while considering a saturated porous medium [2, 3]. In the case of a clear fluid medium, the only one is that conducted lately by Makayssi et al. [4]. All these studies have examined analytically and numerically the effect of the flow behavior index, the Lewis number and the buoyancy ratio on convection heat and mass transfers in the situation where both thermal and solutal buoyancy driven forces act in the same direction (the aiding case)..

Natural convection heat and mass transfer along a vertical plate embedded in a power-law fluid saturated Darcy porous medium in presence of the Soret and Dufour effects is considered by Srinivasacharya and Swamy [5]. It can be concluded according to their analysis that increasing the Soret number (or decreasing the Dufour number) decreases the Nusselt number, but increases the Sherwood number for shear thinning, Newtonian and shear thickening fluids.

The influence of nanoparticles on natural convection boundary layer flow inside a square cavity with water-Al_2O_3nanofluid is accounted by Salma et al. [6]. Various Soret-Dufour coeffcients and Schmidt number have been considered for the flow, temperature and concentration fields as well as the heat and mass transfer rate, horizontal and vertical velocities at the middle height of the enclosure while Pr and Ra are fixed at 6.2, 104 respectively. The results of the numerical analysis lead to the following conclusions: the structure of the fluid streamlines, isotherms and iso-concentrations within the chamber is found to significantly depend upon the Soret-Dufour coeffcients.

Numerical simulation to investigate the effect of heat generation, thermal Rayleigh number, solid volume fraction and Lewis number on flow pattern, temperature field and concentration in a triangular cavity filled porous media saturated Al_2O_3 water nanofluid is conducted by Raju et al. [7]. They found that the heat generation plays an important role on fluid flow pattern, heat and mass transfer and the flow strength is increased for rising the value of heat generation parameter but decrease for increasing values of Lewis number.

Double-diffusive natural convection in a porous arc-shaped enclosure has been numerically studied by Ariyan et al. [8] using Darcy-Brinkman formulation. The impacts of Darcy number, Rayleigh number, Buoyancy ratio, and Lewis number on flow pattern and heat and mass transfer process have been investigated. It was shown for aiding flow ($N < 0$) the strength of the flow is greater than that of opposing flow ($N > 0$). It leads to greater heat and mass transfers for aiding flow case. Any increment in the Darcy number varies heat and mass profiles visibly, as isotherms and iso-concentrations are distributed in the bulk of the cavity for higher Darcy numbers. An increment in the Lewis number results in an improvement/deterioration of mass/heat transfer process.

Unsteady double-diffusive natural convection flow in an inclined rectangular enclosure subject to an applied magnetic field and heat generation parameter is studied by Sabyasachi and Precious [9]. They obtained the average Nusselt numbers and average Sherwood numbers for various values of buoyancy ratio and different angles of the magnetic field by considering three different inclination angles of the enclosure while keeping the aspect ratio fixed. Their results indicate that the flow pattern, temperature and concentration fields are significantly dependent on the buoyancy ratio and the magnetic field angles.

The problem of natural convection in a horizontal fluid layer subject to horizontal gradients of temperature and solute has been solved by both analytical and numerical methods [10]. The influence of the thermal Rayleigh number Ra_T, and parameter a (=0, double diffusive convection; and=1 Soret induced convection) on the intensity of convection were predicted and discussed.

The effects of internal heat generation (IHG), combined effects of Soret and Dufour with variable fluid properties like variable porosity, permeability and viscosity on thermal and diffusion mixed (free and forced) convection flow fluid through porous media over moving surface is analyzed by Girinath and Dinesh [11]. They found that the velocity and temperature profiles decreased for an increase in prandtl number Prwhere as the concentration profile is increased for an increase prandtl number Pr.

Double-diffusive natural convection flow in a trapezoidal cavity with various aspect ratios in the presence of water-based nanofluid and applied magnetic field in the direction perpendicular to the bottom and top parallel walls is studied by Mahapatra et al. [12]. Their results indicated that the strength of vortex decreases/increases as the magnetic field parameter/aspect ratio increases. It was also found that increase in the Rayleigh number causes natural convection due to the increase in the buoyancy forces. In nanofluid, mass transfer ratio was more effective than base fluid.

Authors who drove studies in this domain, made the hypothesis that the porous medium is isotrope and saturated by a newtonian fluid/ / non-newtonian fluid. Anisotropy, which is generally a consequence of a preferential orientation or asymmetric geometry of the grain or fibres, is in fact encountered in all those applications in industry and nature. [13] and others, studied double-Diffusive Natural Convection with Cross-Diffusion Effects in an Anisotropic Porous Enclosure Using ISPH Method, but they considered that the porous medium is saturated by a newtonian fluid. In the present paper we consider that the porous medium (saturated by a non-newtonian fluid) is homogeneous and anisotropic in permeability with arbitrarily oriented principal axes, as seen in nature and many practical applications. An analytical model, based on the parallel flow approximation, is proposed for the case of a shallow layer ($A >> 1$), to determine the effect of anisotropic parameters of the porous matrix on the speed field, the temperature field, the concentration field and the heat transfer.

2. Mathematical Formulation

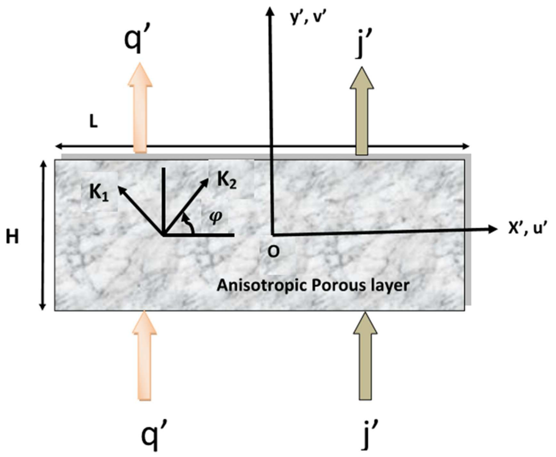

Figure 1. *Physical model and coordinate system.*

The physical system consists of a shallow rectangular cavity field with a porous medium characterized by an anisotropic permeability. The enclosure is of height H and horizontal length L. The generated out-flow is laminaire. The transfer of heat by radiance is negligible. The fluid is binary, non-newtonian and incompressible.

A Cartesian coordinate system is chosen with the x- and y-axes at the geometrical center of the cavity and the y'-axis vertically upward. The top and bottom horizontal boundaries are subject to constant heat (q) and mass (j) fluxes. The porous medium is anisotropic, the permeabilities along the two principal axes of the porous matrix are denoted by K_1 and K_2. The anisotropy of the porous layer is characterized by the permeability ratio $K^*=K_1/K_2$ and the orientation angle φ, defined as the angle between the horizontal direction and the principal axis with the permeability K_2. The continuity, momentum, energy and concentration equations for the porous cavity field are

* Equation governing the conservation of mass:

$$\vec{\nabla} \cdot \vec{V}' = 0 \tag{1}$$

*Equation governing the conservation of momentum (modified Darcy model proposed by ([15, 16])).

$$\vec{V}' = -\frac{\overline{\overline{K}}}{\mu'_a}\left(\vec{\nabla}P' + \rho'\vec{g}\right) \tag{2}$$

*Equation governing the conservation of energy.

$$\sigma'\frac{\partial T'}{\partial t'} + \left(\vec{V}.\vec{\nabla}\right)T' = \alpha_T\vec{\nabla}^2T' \tag{3}$$

*Equation governing the conservation of concentration.

$$\varepsilon'\frac{\partial S'}{\partial t'} + \left(\vec{V}.\vec{\nabla}\right)S' = \alpha_S\vec{\nabla}^2S' \tag{4}$$

*Boussinesq equation.

$$\rho' = \rho_0[1 - (T' - T'_0) - (S' - S'_0)] \tag{5}$$

In these equations, $\vec{V}'$ denotes the velocity vector, p′ the pressure, T ′ the temperature and S′ the concentration. Moreover, μ′a the apparent viscosity, g the gravitational acceleration, T'_0 and S'_0 the constant reference Kelvin temperature and concentration, αS the mass diffusivity in porous medium, ρ_0 the density of the fluid at T'_0, ϱ′ the density, β_T the thermal-expansion coefficient, βS the concentration-expansion coefficient, α_T the thermal diffusivity, ε′ the porosity of the porous medium,. In Eq. (2), the symmetrical second-order permeability tensor $\overline{\overline{K}}$ is defined as

$$\overline{\overline{K}} = \begin{bmatrix} K_1 sin^2\varphi + K_2 cos^2\varphi & (K_2 - K_1)\sin\varphi\cos\varphi \\ (K_2 - K_1)\sin\varphi\cos\varphi & K_2 sin^2\varphi + K_1 cos^2\varphi \end{bmatrix} \tag{6}$$

The boundary conditions of the system are as follows:

$$x' = \pm\frac{L'}{2}\psi' = 0, \frac{\partial S'}{\partial x'} = 0, \frac{\partial T'}{\partial x'} = 0 \tag{7}$$

$$y' = \pm\frac{H'}{2}\psi' = 0, \frac{\partial S'}{\partial x'} = -\frac{j}{\alpha_S}, \frac{\partial T'}{\partial x'} = -\frac{q'}{k} \tag{8}$$

where k is the thermal conductivity and ψ′ the stream function Then, the dimensionless formulation (ψ, T, S) of governing equations become:

$$\left.\begin{aligned} a\frac{\partial^2\psi}{\partial y^2} + 2c\frac{\partial^2\psi}{\partial x\partial y} + b\frac{\partial^2\psi}{\partial x^2} &= -\frac{1}{\mu_a}\left(Z(x,y) + G(x,y)\right) \\ Z(x,y) &= Ra\frac{\partial(T+NS)}{\partial x} + a\frac{\partial\psi}{\partial y}\frac{\partial\mu_a}{\partial y} + c\frac{\partial\psi}{\partial x}\frac{\partial\mu_a}{\partial y} \\ G(x,y) &= c\frac{\partial\psi}{\partial y}\frac{\partial\mu_a}{\partial x} + b\frac{\partial\psi}{\partial x}\frac{\partial\mu_a}{\partial x} \end{aligned}\right\} \tag{9}$$

$$\frac{\partial\psi}{\partial y}\frac{\partial T}{\partial x} - \frac{\partial\psi}{\partial x}\frac{\partial T}{\partial y} = \vec{\nabla}^2T \tag{10}$$

$$\frac{\partial\psi}{\partial y}\frac{\partial S}{\partial x} - \frac{\partial\psi}{\partial x}\frac{\partial S}{\partial y} = \frac{1}{Le}\vec{\nabla}^2S \tag{11}$$

where $Ra=(\rho_0.g.K_1.\Delta T.\beta_T.\ (H/\alpha T)n)/\nu$ the modified thermal Rayleigh number, $N=\beta_S..\Delta S/\beta_T.\Delta T$ the buoyancy ratio, $Le=\alpha_T/\alpha_S$ the Lewis number and ψ is the usual stream function defined as:

$$u = \frac{\partial\psi}{\partial y}, v = -\frac{\partial\psi}{\partial x} \tag{12}$$

such that the mass conservation is satisfied. the constants a, b, and c are defined as.

$$\begin{cases} a = K^* sin^2\varphi + cos^2\varphi, \\ b = sin^2\varphi + K^* cos^2\varphi, \\ c = (1 - K^*)\sin\varphi\cos\varphi\,. \end{cases} \tag{13}$$

It exists few models simulating the out-flow of non-Newtonian fluids in porous medium. While adopting a law of behavior of Ostwald type [14], an expression of the dimensionless viscosity function for a non-Newtonian power-law fluid has been proposed by Pascal. [15, 16] whose expression, in terms of laminar viscosity function, is,

$$\mu_a = \bar{\varepsilon}\left(\left(\frac{\partial\psi}{\partial y}\right)^2 + \left(\frac{\partial\psi}{\partial x}\right)^2\right)^{\frac{n-1}{2}} \tag{14}$$

The dimensionless boundary conditions associated with the no dimensional Eqs. (7) and (8) are

$$x \pm \frac{A}{2}\psi = 0, \frac{\partial S}{\partial x} = 0, \frac{\partial T}{\partial x} = 0, \quad (15)$$

$$y = \pm\frac{1}{2}\psi = 0, \frac{\partial S}{\partial x} = -1, \frac{\partial T}{\partial x} = -1. \quad (16)$$

Were A=L′/H′. The system is then gorvened by seven parameters: the aspect ratio of the cavity, A, the modified thermal Rayleigh number, Ra, the buoyancy ratio, N, the Lewis number, Le, the anisotropic permeability ratio, K*, the orientation angle φ and the power-law index, n.

3. Solution

In large aspect ratios (A >> 1), the present problem can be significantly simplified by the approximation of the parallel flow in which v=0 and u(x, y)=u(y), in the central part of the enclosure. Such an approximation follows from the fact that, for a shallow cavity, the flow in the core of the enclosure is approximately parallel to the horizontal boundaries. The temperature and the concentration field, in the central part, can be divided into the sum of a linear dependence on x and an unknown function of y. Thus, it is assumed that

$$\psi(x, y) = \psi(y) \quad (17)$$

$$T(x, y) = C_T.x + \theta_T(y) \quad (18)$$

$$S(x, y) = C_S.x + \theta_S(y) \quad (19)$$

In the above equations C_T and C_S are the dimensionless temperature gradient and the dimensionless concentration gradient in the x-direction. Substituting Eqs. (17)-(19) into Eqs. (9)–(11), the governing equations can be reduced to the following differential equations:

$$-\frac{d}{dy}\left(\frac{d\psi}{dy}\left(\frac{d\psi}{dy}\right)^{n-1}\right) = \frac{Ra.\xi/cos^2\varphi}{tan^2\varphi+K^*}, \quad (20)$$

$$\frac{d^2\theta_T}{dy^2} = C_T\frac{d\psi}{dy}, \quad (21)$$

$$\frac{d^2\theta_S}{dy^2} = Le.C_S\frac{d\psi}{dy}. \quad (22)$$

In Eq. (20), the constant ξ is defined as: $\xi = C_T + N.C_S$ and the resulting expressions for the velocity, stream function, temperature and concentration fields are given by taking into account the boundary conditions, Eq. (15-16):

3.1. Stream Function

Eq. (20) can be integrated to give the following fully developed Stream function,

$$\psi_n(y) = -\frac{n}{(tan^2\varphi+K^*)^{\frac{1}{n}}}.\frac{(Ra.\xi/cos^2\varphi)^{\frac{1}{n}}}{(n+1).2^{\left(1+\frac{1}{n}\right)}}\left((2y)^{\left(1+\frac{1}{n}\right)} - 1\right) \quad (23)$$

3.2. Velocity Distribution

The velocity profile can be gotten, While drifting Eq. (23):

$$u_n(y) = -\frac{y^{\frac{1}{n}}}{(tan^2\varphi+K^*)^{\frac{1}{n}}}(Ra.\xi/cos^2\varphi)^{\frac{1}{n}} \quad (24)$$

3.3. Temperature Distribution

Eq. (21) can be integrated to give the following fully developed temperature profile,

$$\left.\begin{aligned} T_n(x, y) &= C_T.x - G_1\left(\frac{n.(y)^{\left(1+\frac{1}{n}\right)}}{(2n+1)} - \frac{1}{(2)^{\left(1+\frac{1}{n}\right)}}\right)C_T y - y \\ G_1 &= \frac{n.(Ra.\xi/cos^2\varphi)^{\frac{1}{n}}}{(tan^2\varphi+K^*)^{\frac{1}{n}}.(n+1)} \end{aligned}\right\} \quad (25)$$

3.4. Concentration Distribution

Eq. (22) can be integrated to give the following fully developed concentration function,

$$S_n(x, y) = C_S.x - LeG_1\left(\frac{n(y)^{\left(1+\frac{1}{n}\right)}}{(2n+1)} - \frac{1}{(2)^{\left(1+\frac{1}{n}\right)}}\right)C_S y - y\Bigg\} \quad (26)$$

3.5. Determination of C_T and C_S

The expressions of C_T and C_S can be deduced by integration of the following Eqs. (27) and (28), together with the boundary conditions (15) and (16), by considering the arbitrary control volume of Figure 1 and connecting with the region of the parallel flow [4]. This yields:

$$\int_{-1/2}^{1/2}\left(\frac{d\psi_n}{dy}T_n - \frac{\partial T_n}{\partial x}\right)_{x=0} dy = 0, \quad (27)$$

$$\int_{-1/2}^{1/2}\left(Le.\frac{d\psi_n}{dy}S_n - \frac{\partial S_n}{\partial x}\right)_{x=0} dy = 0. \quad (28)$$

Substituting Eqs. (23)–(26) into Eqs. (27)-(28) and integrating yields, after some straightforward but laborious algebra, an expressions of the form:

$$C_T = \frac{\gamma_1(Ra.\xi/cos^2\varphi)^{\frac{1}{n}}.(tan^2\varphi+K^*)^{\frac{1}{n}}}{(tan^2\varphi+K^*)^{\frac{2}{n}}+\gamma_1\gamma_2(Ra.\xi/cos^2\varphi)^{\frac{2}{n}}} \quad (29)$$

$$C_S = \frac{Le\gamma_1(Ra.\xi/cos^2\varphi)^{\frac{1}{n}}.(tan^2\varphi+K^*)^{\frac{1}{n}}}{(tan^2\varphi+K^*)^{\frac{2}{n}}+\gamma_1\gamma_2 Le^2(Ra.\xi/cos^2\varphi)^{\frac{2}{n}}} \quad (30)$$

were:

$$\gamma_1 = \frac{n(1/2)^{\left(1+\frac{1}{n}\right)}}{2n+1} \quad (31)$$

$$\gamma_2 = \frac{n(1/2)^{(1/n)}}{3n+1} \quad (32)$$

Taking into account ξ=CT + NCS and using the Eqs. (29) - (30) we obtain

$$\varepsilon_1\xi^{\frac{4+n}{n}} + \varepsilon_2\xi^{\frac{2+n}{n}} - \varepsilon_3\xi^{\frac{3}{n}} - \varepsilon_4\xi^{\frac{1}{n}} = f(\xi) \quad (33)$$

The constants ε1, ε2, ε3 and ε4 which depend on Ra, K*, φ, n and Le are given by the following expressions.

$$\left.\begin{aligned}\varepsilon_1 &= (Ra./cos^2\varphi)^{\frac{4}{n}}(Le\gamma_1\gamma_2)^2/(tan^2\varphi + K^*)^{\frac{4}{n}}\\ \varepsilon_2 &= \left(\frac{Ra}{cos^2\varphi}\right)^{\frac{2}{n}}\gamma_1\gamma_2(1+Le^2)/(tan^2\varphi+K^*)^{\frac{2}{n}}\\ \varepsilon_3 &= \left(\frac{Ra}{cos^2\varphi}\right)^{\frac{3}{n}}\gamma_2{\gamma_1}^2(N+Le)/(tan^2\varphi+K^*)^{\frac{3}{n}}\\ \varepsilon_4 &= \left(\frac{Ra}{cos^2\varphi}\right)^{\frac{1}{n}}\gamma_1(1+NLe)/(tan^2\varphi+K^*)^{\frac{1}{n}}\end{aligned}\right\} \quad (34)$$

3.6. Heat Transfer and Mass Transfer

In the case where the cavity is subjected to vertical heat and mass flux per unit area, we define vertical Nusselt and Sherwood numbers, evaluated at x=0 by:

$$Nu_n = \frac{1}{T_n(0,-0.5)-T_n(0,0.5)} \quad (35)$$

$$Sh_n = \frac{1}{S_n(0,-0.5)-S_n(0,0.5)} \quad (36)$$

By substituting Eqs. (25) and (26) in Eqs. (35) and (36), we obtain:

$$Nu_n = \frac{(tan^2\varphi+K^*)^{\frac{1}{n}}}{(tan^2\varphi+K^*)^{\frac{1}{n}}-C_T\gamma_1(Ra.\xi/cos^2\varphi)^{\frac{1}{n}}} \quad (37)$$

$$Sh_n = \frac{(tan^2\varphi+K^*)^{\frac{1}{n}}}{(tan^2\varphi+K^*)^{\frac{1}{n}}-LeC_T\gamma_1(Ra.\xi/cos^2\varphi)^{\frac{1}{n}}} \quad (38)$$

with the following limits

$$\frac{\lim(Sh_n)}{Ra\to 0} = 1,\ \frac{\lim(Nu_n)}{Ra\to 0} = 1. \quad (39)$$

4. Results and Discussion

4.1. Case of a Non-newtonian Fluid Saturating Anisotropic Porous Medium such as (φ=0°)

When the principal axes of the porous matrix (K_1, K_2) coincides with the axial (Ox,Oy), we have φ=0°, cos(φ)=1, tan(φ)=0 and Eq. (23) - (26) Become:

$$\psi_n(y) = -\frac{n}{(K^*)^{\frac{1}{n}}}\cdot\frac{(Ra.\xi)^{\frac{1}{n}}}{(n+1).2^{\left(1+\frac{1}{n}\right)}}\left((2y)^{\left(1+\frac{1}{n}\right)}-1\right) \quad (40)$$

$$u_n(y) = -\frac{y^{\frac{1}{n}}}{(K^*)^{\frac{1}{n}}}(Ra.\xi)^{\frac{1}{n}} \quad (41)$$

$$T_n(x,y) = C_T.x - \frac{n.(Ra.\xi)^{\frac{1}{n}}}{(K^*)^{\frac{1}{n}}.(n+1)}\left(\frac{n.(y)^{\left(1+\frac{1}{n}\right)}}{(2n+1)} - \frac{1}{(2)^{\left(1+\frac{1}{n}\right)}}\right)C_Ty - y \quad (42)$$

$$S_n(x,y) = C_S.x - Le\frac{n.(Ra.\xi)^{\frac{1}{n}}}{(K^*)^{\frac{1}{n}}.(n+1)}\left(\frac{n(y)^{\left(1+\frac{1}{n}\right)}}{(2n+1)} - \frac{1}{(2)^{\left(1+\frac{1}{n}\right)}}\right)C_Sy - y \quad (43)$$

4.2. Case of a Non-newtonian Fluid Saturating Isotropic Porous Medium

When the permeability is the same in all directions (i.e. for an isotropic porous layer), we have: K_1=K_2. Which implies that K*=1. The above result (Eq. 40-43), in the case K*=1, reduces to

$$\psi_n(y) = -\frac{n.(Ra.\xi)^{\frac{1}{n}}}{(n+1).2^{\left(1+\frac{1}{n}\right)}}\left((2y)^{\left(1+\frac{1}{n}\right)}-1\right) \quad (44)$$

$$u_n(y) = -y^{\frac{1}{n}}(Ra.\xi)^{\frac{1}{n}} \quad (45)$$

$$T_n(x,y) = C_T.x - \frac{n.(Ra.\xi)^{\frac{1}{n}}}{(n+1)}\left(\frac{n.(y)^{\left(1+\frac{1}{n}\right)}}{(2n+1)} - \frac{1}{(2)^{\left(1+\frac{1}{n}\right)}}\right)C_Ty - y (46)$$

$$S_n(x,y) = C_S.x - Le\frac{n.(Ra.\xi)^{\frac{1}{n}}}{.(n+1)}\left(\frac{n(y)^{\left(1+\frac{1}{n}\right)}}{(2n+1)} - \frac{1}{(2)^{\left(1+\frac{1}{n}\right)}}\right)C_Sy - y \quad (47)$$

which is reported in the past by Benhadji and Vasseur (2001).

4.3. Case of Newtonian Fluid Saturating Anisotropic Porous Medium

By introducing into Eq. (23)– (26), n=1, we obtain:

$$\psi_1(y) = -\frac{(Ra.\xi/cos^2\varphi)}{2(tan^2\varphi+K^*)}\cdot\left(y^2-\frac{1}{4}\right) \quad (48)$$

$$u_1(y) = -\frac{(Ra.\xi/cos^2\varphi)}{(tan^2\varphi+K^*)}y \quad (49)$$

$$T_1(x,y) = C_T.x - \frac{(Ra.\xi/cos^2\varphi)}{2(tan^2\varphi+K^*)}\left(\frac{y^2}{3}-\frac{1}{4}\right)C_Ty - y, \quad (50)$$

$$S_1(x,y) = C_S.x - Le\frac{(Ra.\xi/cos^2\varphi)}{2(tan^2\varphi+K^*)}\left(\frac{y^2}{3}-\frac{1}{4}\right)C_Sy - y \quad (51)$$

4.4. Case of Newtonian Fluid Saturating Isotropic Porous Medium

When the permeability is the same in all directions (i.e. for an isotropic porous layer), we have: K_1=K_2. Which implies that K*=1. The above result (Eq. 48 - 51), in the case K*=1 and φ=0°, reduces to

$$\psi_1(y) = -\frac{Ra.\xi}{2}\cdot\left(y^2-\frac{1}{4}\right), \quad (52)$$

$$u_1(y) = -Ra.\xi.y, \quad (53)$$

$$T_1(x,y) = C_T.x - \frac{Ra.\xi}{2}\left(\frac{y^2}{3}-\frac{1}{4}\right)C_Ty - y, \quad (54)$$

$$S_1(x,y) = C_S.x - \frac{Le.Ra.\xi}{2}\left(\frac{y^2}{3}-\frac{1}{4}\right)C_Sy - y. \quad (55)$$

These results are in agreement with the solutions obtained in the past by AMARI et al. and KALLA et al. [17, 19].

4.5. Effect of Anisotropy Parameters on Heat Transfer and Mass Transfer

The determination of the constants C_T and C_S depends on the solution of the equation f (ξ)=0. A programming using the Fortran software is done and allowed us to draw the curve (figure 2). This curve indicates in case of a Newtonian fluid (n=1), three solutions namely: ξ=0, ξ=0.3213 and ξ=0.9337.

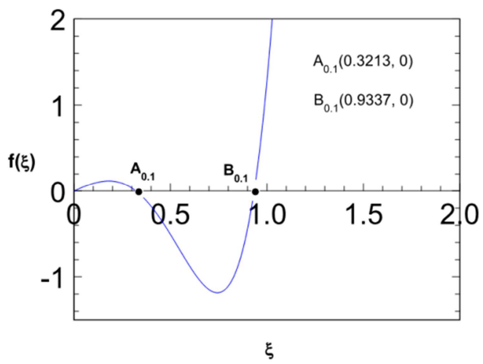

Figure 2. *Solution of f (ξ)=0.*

The effect of varying of Ra, the Rayleigh number and of K*, the permeaility ratio on the Sherwood number, Sh, is illustrated in Figure 3 for n=1, ξ=0.3213, Le=4 and φ=0°. It observes that when the Rayleigh number increases, the Sherwood number for mass transfer increases too. It is also observed that for low values of the Rayleigh number, the effect of anisotropy is also low. In other words, upon increasing Ra, the effect of anisotropy becomes more and more important. This is explained by the fact that when the Rayleigh number tends towards to zero, the sherwood number tends towards unity (Eq. 39). Figure 3 also shows that the anisotropy ratio K* has a great influence on the Sherwood number. Indeed, the anisotropic ratio K* decreases with an increase of the Sherwood number, Sh. Moreover, compared to isotropic situation (K*=1) the Sherwood number for mass transfer is enhanced when K* < 1, and decreased when K* > 1. It results then, when the principal axes of anisotropy are oriented in a direction coinciding with the coordinate axes (i.e., φ=0°), the Sherwood number for mass transfer increases (or decreases) when the permeability in the vertical direction (K1) is smaller (or higher) than the permeability in the horizontal direction (K2).

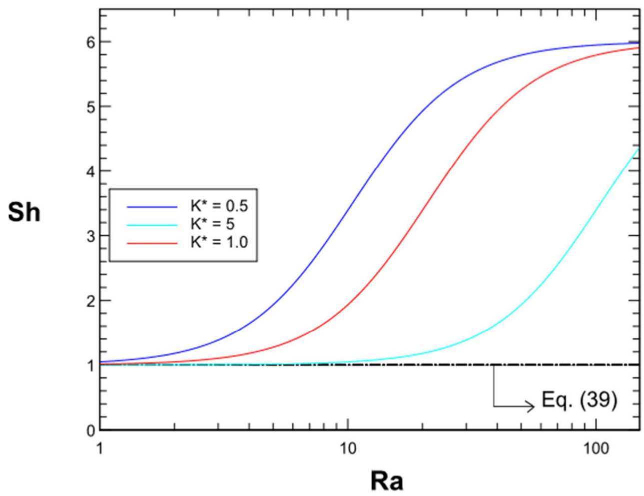

Figure 3. *The effect of varying of Ra, the Rayleigh number and of K*, the permeaility ratio on the Sherwood number, Sh.*

The effect of the anisotropic angle φ and of the Rayleigh number, Ra, on the Sherwood number for mass transfer, Sh, is illustrated in Figure 4 when n=1, ξ=0.3213, Le=4 and K*=0.5. It is seen that for a given value of the Rayleigh number, the Sherwood number increases with the decrease of the anisotropic angle φ when the permeability ratio is made smaller than 1 (i.e., K*< 1).

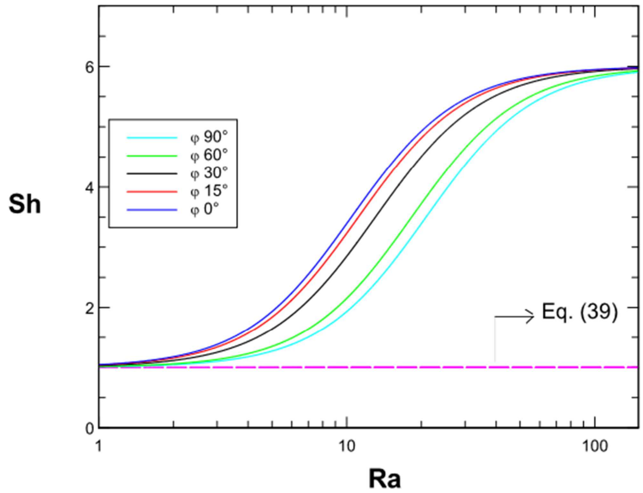

Figure 4. *The effect of the anisotropic angle φ and of the Rayleigh number, Ra, on the Sherwood number for mass transfer, Sh.*

Independently of φ and K*, the Sherwood number for mass transfer increases with the increase of Rayleigh number. For φ=90°, the Sherwood number is minimal and maximal when φ=0°. It is evident from the analysis of this result that the characteristic parameter of the mass transfer (Sh) is minimal (or maximal) when the main axis having the most elevated permeability of the porous layer is perpendicular (or parallel) to the gravity. On the other hand, results illustrated in Figure 5 show that, when the permeability ratio is made superior than 1 (i.e., K* > 1), for φ=0°, the Sherwood number is minimal and maximal when φ=90°.

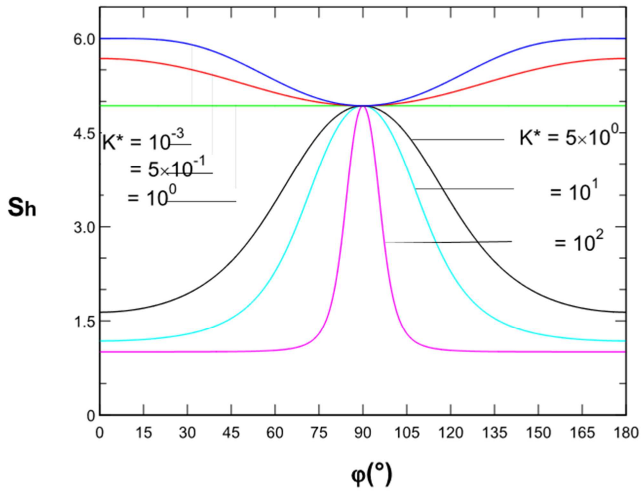

Figure 5. *Effect of the anisotropic angle φ and of K*, on the Sherwood number for mass transfer, Sh.*

The evolution of the Nussselt number according to the Rayleigh number and for different values of K* when n=1, ξ=0.3213, Le=4, and φ=0◦, is illustrated in Figure 6. The results show that Nusselt number is an increasing function of the Rayleigh number. Then, compared to isotropic situation (K*=1) and for a given value of Rayleigh number, the Nussselt number for heat transfer is enhanced when K* < 1, and decreased when K* > 1. It results then, when the principal axes of ani-sotropy are oriented in a direction coinciding with the coordinate axes (i.e., φ=0°), the enhanced for heat transfer increases (or decreases) when the permeability in the vertical direction (K1) is smaller (or higher) than the permeability in the horizontal direction (K2). Otherwise, results illustrated in Figure 7 show that, when the permeability ratio is made superior than 1 (i.e., K* > 1), for φ=0°, the Nussselt number for heat transfer is minimal and maximal when φ=90°.

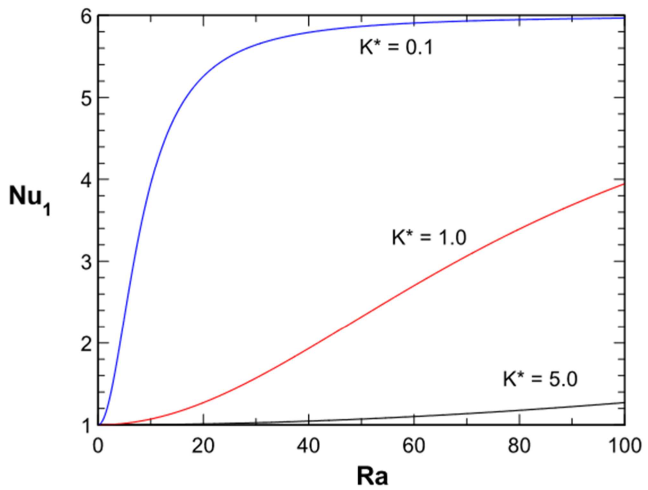

Figure 6. *Evolution of the Nussselt number according to the Rayleigh number and for different values of K*.*

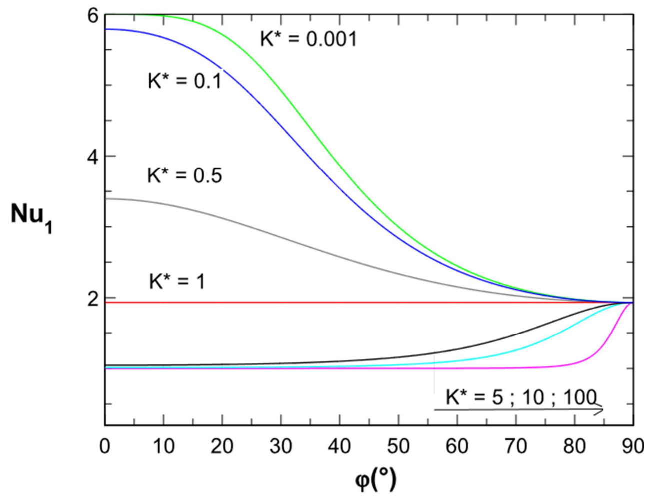

Figure 7. *Effect of the anisotropic angle φ and of K*, on the Nusselt number.*

5. Conclusion

In this investigation, an analytical study of heat and mass transfer is studied in two-dimensional horizontal shallow enclosure, filled with non-Newtonian power-law fluids. Our research concerns the influence of hydrodynamic anisotropy on the heat and mass transfer. An analytical model, based on the parallel flow approximation, is proposed for the case of a shallow layer (A >> 1), to determine the effect of anisotropic parameters of the porous matrix on the speed field, the temperature field, the concentration field and the heat transfer. The main conclusions of the present study are:

The Sherwood number for mass transfer is an increasing function of the Rayleigh number.

Compared to isotropic situation (K*=1) the Sherwood number for mass transfer is enhanced when K* < 1, and decreased when K* > 1.

The characteristic parameter of the mass transfer (Sh) is minimal (or maximal) when the main axis having the most elevated permeability of the porous layer is perpendicular (or parallel) to the gravity.

The enhanced for heat transfer increases (or decreases) when the permeability in the vertical direction (K_1) is smaller (or higher) than the permeability in the horizontal direction (K_2).

References

[1] Jaluria, Y. (2003). Thermal processing of materials: From basic research to engineering. Journal of Heat Transfer 125, 957-979.

[2] Getachew, D., D. Poulikakos and W. J. Minkowycz. 1998. "Double-diffusive in a porous cavity saturated with non-Newtonian Fluid". Journal of Thermophysics and Heat Transfer 12, 437-446.

[3] Benhadji, K. and P. Vasseur. 2001. "Double diffusive convection in a shallow porous cavity filled with a non-Newtonian fluid". International Communications in Heat and Mass Transfer 28, 763-772.

[4] Makayssi, T., M. Lamsaadi, M. Nami, M. Hasnaoui, A. Raji and A. Bahlaoui. 2008. "Natural double-diffusive convection in a shallow horizontal rectangular cavity uniformly heated and salted from the side and filled with non-Newtonian power-law fluids: the cooperating case", Energy conversion and Management 49, 2016-2025.

[5] Srinivasacharya, D., Swamy Reddy, G. 2012. Double Diffusive Natural Convection in Power-Law Fluid Saturated Porous Medium with Soret and Dufour Effects J. of the Braz. Soc. of Mech. Sci. Eng. Vol. XXXIV, No. 4, pp. 525-530.

[6] Salma Parvin, Rehena Nasrin, Alim, M. A., Hossain, N. F. 2013 Double diffusive natural convective flow characteristics in a cavity Procedia Engineering Vol. 56, pp. 480 488.

[7] Raju Chowdhury, Salma Parvin, and Md. Abdul Hakim Khan. 2016. Finite element analysis of double-diffusive natural convection in a porous triangular enclosure filled with Al_2O_3-water nanofluid in presence of heat generation Heliyon. 2016 Aug; 2 (8): e00140.

[8] Ariyan Zare Ghadi, Ali Haghighi Asl, Mohammad Sadegh Valipour. 2014. Numerical modelling of double-diffusive natural convection within an arc shaped enclosure filled with a porous medium Journal of Heat and Mass Transfer Research Vol. 1 pp. 83-91.

[9] Sabyasachi Mondal and Precious Sibanda. 2016. An Unsteady Double-Diffusive Natural Convection in an Inclined Rectangular Enclosure with Different Angles of Magnetic Field International Journal of Computational Methods, Vol. 13, No. 041641015.

[10] BIHICHE, K., LAMSAADI, M., NAMI, M., ELHARFI, H., KADDIRI, M., LOUARAYCHI, A. 2017. Double-diffusive and Soret-induced convection in a shallow horizontal layer lled with non-Newtonian power-law uids 13me Congrs de Mcanique 11 - 14 Avril 2017 (Mekns, MAROC).

[11] Girinath Reddy, M., Dinesh, P. A. 2018. Double Diffusive Convection and Internal Heat Generation with Soret and Dufour Effects over an Accelerating Sur- face with Variable Viscosity and Permeability Advances in Physics Theories and Applications, Vol. 69, pp. 7-25.

[12] Mahapatra, T. R., Saha, B. C. Pal, D. 2018 Magnetohydrodynamic double- diffusive natural convection for nanofluid within a trapezoidal enclosure. Comp. Appl. Math. 37, 61326151 (2018) doi: 10.1007/s40314-018-0676-5.

[13] Abdelraheem M. Aly and Mitsuteru Asai (October 22nd 2015). Double- Diffusive Natural Convection with Cross-Diffusion Effects in an Anisotropic Porous Enclosure Using ISPH Method, Mass Transfer - Advancement in Process Modelling, Marek Solecki, Intech Open, DOI: 10.5772/60879.

[14] Ostwald, W. 1925. “Ueber die Geschwindigkeitsfunktion der Viskositat Disperser Système”, L, Kolloïd-Z, Vol. 36, pp. 99-117.

[15] PASCAL, H. 1983. “Rheological Behaviour Effect of Non Newtonian Fluids on Steady and Unsteady Flow Through a Porous Media”, International Journal for Numerical and Analytical Methods in Geomechanics, vol. 7, pp. 289-303.

[16] PASCAL, H. 1986. “Rheological effects of Non Newtonian Behaviour of Displacing Fluids on Stability of a Moving Interface in Radial Oil Displacement Mechanism in Porous Media”, International Journal Engineering Science, vol. 24, No. 9, pp. 1465-1476.

[17] AMARI, B., VASSEUR, P., and BILGEN, E. 1994. “Natural Convection of Non Newtonian Fluids in a Horizontal Porous Layer”, Wrme-und Stoffbertragung, vol. 29, pp. 185-193.

[18] MAMOU, M., VASSEUR, P., BILGEN, E., and GOBIN, D. 1995. “Double- Diffusive Convection in an Inclined Slot Filled with Porous Medium”, Eur. J. Me- chanics, B/Fluids, vol. 14, pp. 629-652.

[19] KALLA, L., MAMOU M., VASSEUR, P. and ROBILLARD, L. 1999. “Mul- tiple Steady States for Natural Convection in a Shallow Porous Cavity Subject to Uniform Heat Fluxes”, International Communications in Heat Mass Transfer, vol. 26, No. 6, pp. 761-770.